Journal of Archaeological Method and Theory (2024) 31:2053–2081
https://doi.org/10.1007/s10816-024-09664-7

RESEARCH

Rethinking Wear Rate Analysis: a New Dentin Exposure Proxy and its Applications to Ancient Chinese Populations

Shiyu Yang[1,2,7] · Laura M. Martínez[2,3] · Alejandro Romero[4] · Susana Carrascal[2,3,5] · Jie Guo[1] · Albert E. Dyowe[6] · Quanchao Zhang[1] · Alejandro Pérez-Pérez[2,3]

Accepted: 30 July 2024 / Published online: 16 August 2024

Abstract

Assessing age through dentin exposure often leads to underestimated age due to assumptions of constant molar wear rate. New methods for age-related dentin exposure accrual could facilitate cross-population comparisons independent of dietary habits and sociocultural strategies. We analyzed 3D dentin exposure surfaces in four Chinese archaeological samples to reveal variations in dentin exposure rates linked to socioeconomic practices. Linear regression models of dentin exposure areas across molar rows showed significant correlations, with the first molars exhibiting steeper slopes and smaller intercepts compared to the second molars, which had intermediate values, and the third molars showing the highest intercepts and lowest slopes. The first molar contributed most to overall dentin exposure in the molar quadrant, while the second molar wore faster post-eruption. Among populations, Banlashan, predominantly agriculturalist; Houtaomuga, focused on fishing; and Jiayi, a nomadic hunting society, displayed similar wear rate patterns. In contrast, Dunping, a Bronze Age nomadic settlement situated on a high-altitude plateau, exhibited distinctively lower wear rates. These observed dentin exposure rates aligned with ecological and dietary constraints, enabling interpopulation comparisons using the proposed 3D dentin exposure proxy. Moreover, the statistical model allows for comparing wear rates across populations relative to dietary habits and potentially estimating age at death for isolated archaeological specimens, whether humans or animals. The precision of this physiological age estimation depends on the regression models used, necessitating further research with specimens of known age at death.

Keywords Dentin exposure · Wear rates · Age at death · Northern China · Neolithic to early Bronze Age

Quanchao Zhang and Alejandro Pérez-Pérez contributed equally to this work.

Extended author information available on the last page of the article

Introduction

Dental wear is a physiological, age-dependent process of gradual enamel loss and dentin exposure largely determined by dietary abrasiveness (Kaifu et al., 2003; Romero et al., 2019). After the dental crown reaches full functional occlusion, enamel surfaces progressively wear down due to tooth-to-tooth attrition and tooth-to-food abrasion. These processes involve hard, microscopic particles from both intrinsic sources, such as silica-based phytoliths from edible monocotyledon plants, and extrinsic sources, such as gritty particles incorporated into food during processing (Lucas & van Casteren, 2015; Schmidt, 2010).

Traditional wear scoring systems rely on discrete cusp enamel wear and dentin exposure stages (Broca, 1879; Murphy, 1959). Gross dental wear scores on molar teeth allow classifying individuals into broad age categories (Lovejoy, 1985). However, age estimations based on discrete scores of dentin exposure (Gilmore & Grote, 2012) tend to underestimate actual individual ages (Miles, 2001), since they frequently assume constant molar wear rates, independent of the population's lifestyle and diet (Brothwell, 1963). Overall, in populations with low wear rates, dentin exposure scores were expected to provide less accurate age estimations because interindividual variation in wear could obscure the age-related signal (Cuesta-Torralvo et al., 2021; Gilmore & Grote, 2012).

The dentitions of geographically and temporally diverse prehistoric hunter-gatherer populations exhibited higher wear scores than those of agriculturalist groups due to their less refined, tougher foods consumed (Deter, 2009; Kaifu et al., 2003). Furthermore, dietary proclivities and technical methods of food processing induced significant variation in the percentages of dentin exposure in both Arctic (Clement & Hillson, 2012; Górka et al., 2016) and mesothermal (Richards & Brown, 1981; Romero et al., 2019) hunter-gatherers. Although molar crown shape changes with age due to wear, the models were likely ineffective for determining wear rates and age at death in skeletal remains because of the high variability in molar wear within modern human populations (Benazzi et al., 2008; Cuesta-Torralvo et al., 2021). Smith (1984) also noted that the angle of the occlusal plane of molar teeth was sensitive to interpopulation differences in food toughness, independent of the variation in wear scores. Notwithstanding the age and diet interdependence, making inferences of age at death or dietary habits based on molar wear rates required that one of the two factors remain constant (Rose & Ungar, 1998: 352). In this context, we need novel methods to estimate dentin exposure rates, rather than averaging measures of dental wear scores of skeletal samples for which the age distribution is unknown.

In this study, we employed a three-dimensional (3D) dentin exposure analysis approach, using a continuous measure of dentin exposure on molar tooth rows (M_1-M_2-M_3). This enabled us to derive wear rates through regression models of dentin exposure, allowing for comparisons among archaeological populations.

Materials and methods

We studied human skeletal remains from the Chinese prehistoric sites of Houtaomuga, Banlashan, Dunping, and Jiayi, curated in the *Human Skeletal Collections* at the School of Archaeology (Jilin University, China). The total sample analyzed consisted of 275 individuals (52.1% of the available skeletons), including 107 females, 137 males, and 31 subadult unsexed individuals (Table 1). The variation in sample sizes across sites resulted from differences in skeletal preservation and environmental conditions affecting the burials. Detailed criteria for sample selection are outlined in the sample processing section. The remains from the Jiayi cemetery, located in an extremely arid desert environment, were better preserved than those from Houtaomuga, placed close to a river margin with moist soils. Specimens lacking erupted permanent molars or not in functional occlusion were excluded from the study sample. The proportion of infants lacking erupted first molars was higher in Houtaomuga compared to the other sites (Xiao, 2014). We chose permanent, fully erupted mandibular molars (M_1, M_2, and M_3) with measurable patches of occlusal dentin exposure.

Before this research, skeletal samples from Banlashan and Dunping were aged and sexed by one of us (SY) using a combination of skeletal markers. These included dental eruption patterns, decay stages of the pubic symphysis and ilium auricular surfaces, cranial suture closure stages, and upper and lower limb bone epiphyseal fusion. The standard skeletal markers we employed are described by Buikstra and Ubelaker (1994), as well as for Chinese skeletal remains by Wu et al. (1984) and Shao (1985). These markers are also detailed by He (2015) and Xiao (2014).

Archaeological and Ecological Background

Around 5500 BCE, during the Late Neolithic, a significant cooling event occurred in the ecologically fragile zone of northern China. This event stimulated the development of agricultural practices, marked by the introduction of tools such as stone plows (Teng, 2013). However, in the Great Wall area, subsistence patterns gradually

Table 1 Available skeletal and dental samples by site, sex, and tooth type

Site	Period	ka BP	N_t	N_s				N_m ($D>0$)			
				♀	♂	?	All	M_1	M_2	M_3	All
Houtaomuga A	Neolithic	12–2.7	29	1	9	3	13	11	9	1	21
Banlashan	Neolithic	7.5–5	44	16	8	1	25	17	11	–	28
Dunping	Bronze	2.5–2.3	83	22	40	0	62	16	8	–	24
Houtaomuga B	Bronze-Iron Age	2.7–1.7	88	15	23	1	39	34	27	5	66
Jiayi	Bronze-Iron Age	2.8–2.3	284	53	57	26	136	100	69	20	189
		All	528	107	137	31	275	178	124	26	328

ka BP thousands of years before present, *Nt* total number of burials, *Ns* well-preserved individuals by sex, *Nm* dental sample of lower molar teeth with dentin exposure ($D>0$)

Fig. 1 Map of Chinese provinces indicating the location of the four sites studied: Houtaomuga (Neolithic to Liao and Jin dynasties, 12,000 BCE–1781 ACE, Jilin Province), Banlashan (Late Neolithic, 3200–3050 BCE, Liaoning Province), Dunping (Bronze Age, 546–283 BCE, Gansu Province), Jiayi (Late Bronze to Early Iron Age, 800–300 BCE, Xinjiang Province)

shifted from agriculture to a nomadic lifestyle during the transition from the Neolithic to the Bronze Age. Eventually, animal husbandry became the predominant economic strategy in many regions (Yang & Cao, 2007). During this transition, human populations from northern China exhibited a wide gradient in subsistence patterns, ranging from the nomadic civilizations of the Eurasian grasslands to the agricultural civilizations of the Central Plains. The dietary habits of these ancient populations varied greatly in terms of food consistency and abrasive potential. Both Dunping and Jiayi had nomadic economies, but their geographical environments and ecological constraints were completely different.

The Houtaomuga cemetery is located on the shores of Xinhuang Lake in Yonghe Village, Da'an City, in Jilin Province, south of the Songnen Plain, close to the intersection of the Nenjiang and Songhua rivers (Fig. 1). From an archaeological perspective, the Houtaomuga site spans seven phases, from the Early Neolithic period (12,000 BCE) to the Liao and Jin dynasties (960–1279 ACE) (Wang, 2018; Xiao, 2014). The subsistence strategy in northeastern China during the Neolithic was mainly based on fishing activities (Gao, 2021; Zhu, 2019). Carbon and nitrogen stable isotopic analyses (^{13}C, ^{15}N) indicated that freshwater fish were the major component of the diet of Houtaomuga during the Neolithic (A phase) (Kunikita et al., 2017). However, during the Bronze to the Early Iron Age (2700 BCE–1781 ACE), Houtaomuga (B phase) showed a nomadic lifestyle, mostly based on animal husbandry and seasonal harvesting (Kunikita et al., 2017; Wang, 2018; Xiao, 2014).

The Banlashan site is a Late Neolithic rubble mound cemetery located at Chaoyang in Liaoning Province in northeastern China (Fig. 1). It dates back to 3200–3050 BCE and belongs to the late period of the Hongshan culture. Analyses of ^{13}C and ^{15}N of the human skeletons suggested that the Banlashan people mainly consumed C4 plant foods and/or animals that ate C4 plants while few wild C3 plants were consumed and animal protein accounted for a high proportion of their diet (Zhang et al., 2017a, 2017b). Paleo-ethnobotany and zoo-archaeology studies have shown that foxtail millet (*Setaria italica*) and proso millet (*Panicum miliaceum*) were widely cultivated and were the main sources of plant foods (Sun & Zhao, 2013; Sun et al., 2016). Fishing, hunting of wild boars, deer and rabbits, and domestic pig livestock also occupied a significant portion of their food procurement activities (Chen, 2014; Suo & Li, 2013).

The Dunping cemetery in Zhang County in Gansu Province (Fig. 1), situated on a plateau with an altitude ranging between 2000 and 3000 m, is surrounded by mountains, rivers, and valleys (Mao et al., 2019). The environment in this area was highly diverse, with overall cold and dry climatic conditions, although the valley alluvial plains were expansive and lush (Jiang, 2011). The Dunping population occupied an array of ecosystems differing in land formation, climatic conditions, and natural resource availability. The archaeological assemblage of the Dunping cemetery belongs to the West-Rong culture system of the northern Bronze culture belt in the Warring States period, dated by ^{14}C to 546–283 BCE, a transitional period from a nomadic tradition to a farming culture (Mao et al., 2017, 2019).

The Jiayi population, located in the Turpan basin deep within the interior of the Eurasian continent, experienced extreme drought, high temperatures, and frequent sandstorms (Cheng et al., 2006), which favored fast-drying foods. The nomadic Jiayi population processed foods without water, resulting in hard, long-term preservation, and easy-to-carry *Ta-er-mi* (塔尔米) traditional food. This food was the preferred for migrating herdsmen (Liu et al., 2009), as also documented at the Yanghai cemetery (Liu, 2020) in Xinjiang, along the Silk Road, where unearthed tools were consistently used for processing coarse foods such as *Mi* cake (糜饼) and millet. The Jiayi cemetery in Turpan, Xinjiang Province (Fig. 1), has been dated to 800–300 BCE, both by typology and ^{14}C AMS (Wang, 2017; Xiao, 2018), from the *Subeixi* Late Bronze Age to the Early Iron Age archaeological cultures in the Xinjiang Uygur Autonomous Region. It is the only prehistoric culture found in the Turpan basin. Numerous tools have indicated a mainly hunting economy with small-scale farming (Wang et al., 2014). Environmental studies on Jiayi cemetery identified 14 plant remains, including weeds, such as wild foxtail millet (*Setaria viridis*), common reed (*Phragmites australis*), cockspur grass (*Echinochloa crusgalli*), and grains such as barley (*Hordeum vulgare*) and common millet (*Panicum miliaceum*). This evidence suggests that the Jiayi population supplemented their mainly nomadic and hunting economy with a small proportion of agricultural planning (Jiang et al., 2021; Li et al., 2013). The vegetation of northeastern China is highly sensitive to variations in the East Asian Monsoon (Zhou et al., 2002). Low-temperature events occurred eight times from 9200 to 600 cal. BP (Li et al., 2011). These events led to climatic

Fig. 2 Meshes of selected molar quadrants (M_1-M_2-M_3 from left to right) from adult individuals at Jiayi, ▶ displaying dentin exposure (red surfaces) ranging from lightly worn (top) to heavily worn (bottom). The wear score (WS) according to Smith's (1984), areas of dentin exposure (*D*) by tooth type, and the total sum of dentin exposure areas for the quadrant (*S*) are depicted. Specimen reference numbers and estimated age (years) are included; WS and *D* values for each tooth are indicated under respective molars. Mesial (left); buccal (top)

instability that may have contributed to changes in economic, social, and cultural conditions, as well as in the pathogen milieu. This could explain the high prevalence of linear enamel hypoplasia (Chen & Rong, 1998) observed in the Houtaomuga population, with an incidence of up to 72.73% during phases II and IV (Merrett et al., 2016; Xiao, 2014).

Sample Processing and Measuring

We molded dental quadrants, including lower molar teeth, following standardized protocols (Galbany et al., 2006) with 3M™ light-body polyvinylsiloxane impression material. We used Feropur PR55 polyurethane by Feroca™ for the positive casts of the molar teeth. Before polymerization, we centrifuged the molds for approximately 1 min at 800 rpm to prevent the formation of air bubbles. We obtained digital 3D meshes of all molar quadrants using a 3D EinScan SP2 Shinning™ scanner in *non-texture* mode, capturing eight scans per quadrant at 45° angles. We scanned each cast three times, capturing occlusal, buccal, and lingual views, and automatically fused them using the *surface topography* mode into a single point-cloud mesh. Afterward, we applied a slight smoothing filter to eliminate outlier points and exported the meshes to both a polygon (PLY) and an ASCII object (OBJ) file formats.

We derived two measures of occlusal dentin exposure for each molar tooth: a wear score (WS), recorded from the original molar using the eight-stage classification by Smith (1984), and the area of the dentin exposure surfaces on each molar (*D*, mm^2) (Fig. 2) using the *Shining* digital software. Additionally, we computed the overall sum of the dentin exposure surfaces for the molars in a mandibular quadrant ($S = D_{M1} + D_{M2} + D_{M3}$, mm^2). Both *D* and *S* represent 3D measures of surface topography and are measured in square millimeter units. We assigned an *S* value for a given quadrant only when the specimen met three conditions. First, the M_1 tooth had to be present and show dentin exposure; otherwise, we discarded the complete specimen. This condition allows the inclusion of subadult individuals in the sample, provided they have a fully erupted and worn first molar. Note that the focus is on the permanent molar tooth, not the individual. Secondly, the M_2 tooth was either present, showing or lacking dentin exposure (the absence of dentin exposure was recorded as a zero *D* value), or it had not yet erupted, in which case a zero *D* value was assigned. Third, and last, the M_3 was either present (in which case the M_2 should also be present) or absent exclusively due to not having yet erupted. We recorded a zero *D* value for the lack of dentin exposure in an observable molar tooth, while we considered a missing value when the tooth was absent not because of a lack of eruption. When a tooth row showed a missing value due to the absence of one or more molar teeth, and the cause of that absence was not attributed to non-eruption, we discarded

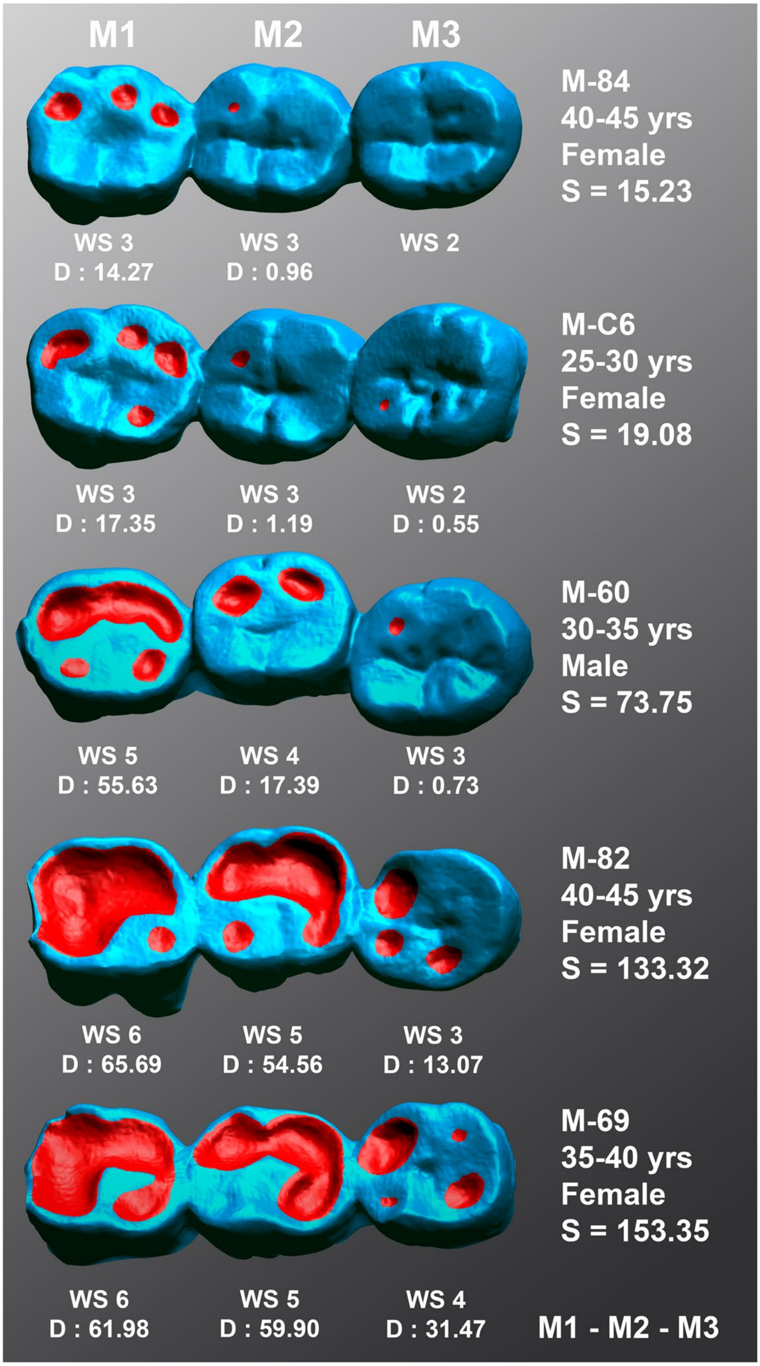
M1
M2
M3
M-84
40-45 yrs
Female
S = 15.23
WS 3
D : 14.27
WS 3
D : 0.96
WS 2
M-C6
25-30 yrs
Female
S = 19.08
WS 3
D : 17.35
WS 3
D : 1.19
WS 2
D : 0.55
M-60
30-35 yrs
Male
S = 73.75
WS 5
D : 55.63
WS 4
D : 17.39
WS 3
D : 0.73
M-82
40-45 yrs
Female
S = 133.32
WS 6
D : 65.69
WS 5
D : 54.56
WS 3
D : 13.07
M-69
35-40 yrs
Female
S = 153.35
WS 6
D : 61.98
WS 5
D : 59.90
WS 4
D : 31.47
M1 - M2 - M3

the entire quadrant and did not assign an S value. We treated each quadrant as an independent specimen to maximize sample sizes and because bilateral differences in dentin exposure within individuals are not likely to affect the regression models.

Statistical Modeling of Dentine Exposure

We refrained from conducting direct statistical comparisons of dentin exposure metrics between samples because the wear is an age-related variable that strongly depends on the age distribution of the skeletal samples considered. Instead, we developed least square regression models (Linear, Quadratic, and Power) of D onto both WS and S to analyze the regression of the two scoring proxies (WS and D) and to assess the contribution of the continuous measure of dentin exposure to the overall dentin exposure of the molar quadrant. Additionally, we used nonlinear regression models (Compound and Power) to examine the association between the estimated skeletal age (Age) and the 3D dentin exposure (D). Finally, we employed a Power regression model of D onto S (Eq. (1)) to estimate the relative contribution of each molar to the overall dentin exposure of the mandibular quadrant.

$$S = a\,D^b \tag{1}$$

$$\ln S = \ln a + b \ln D \tag{2}$$

This choice was made because the Power function can be directly transformed into a Linear function (Eq. (2)) by taking the logarithm (in this case, the natural logarithm) of the two variables ($\ln D$, $\ln S$). The intercept ($\ln a$) predicts the $\ln S$ value attained at the onset of the dentin exposure contribution of each molar tooth, and the slope (b) reflects the rate at which $\ln D$ contributes to the overall dentin exposure $\ln S$.

A physiological age (E) of an individual (based on the overall dentin exposure S) can be estimated if a significant regression model can be obtained between E and S. For this purpose, we tested several models and finally selected a linear one (Eq. (3)). By combining Eqs. (1) and (4), we can estimate a model-based age at death from the dentin exposure of each molar (Eq. (3)), as well as the expected dentin exposure (D) at any given age (Eq. (4)). Note that E is not the actual age at death of an individual but a predicted physiological age based on a given dentin exposure.

$$E = c + bS = c + baD^b \tag{3}$$

$$D = \sqrt[b]{\frac{E - c}{ba}} \tag{4}$$

Dentin Exposure Rates

From the ln-transformed Linear regression models of the three molars, we deduced average population overall wear rates for the age intervals between the onsets of dentin exposure for two consecutive molars. These age intervals, derived from molar eruption ages in modern *Homo sapiens* (Ash & Nelson, 2003), were a juvenile 6-year interval, from M_1 (5.5 years) to M_2 (11.5 years), and a subadult 7-year interval, from M_2 (11.5 years) to M_3 (18.5 years). Gilmore and Grote (2012) provide slightly smaller estimates of the age intervals: a 5.29-year juvenile interval for an average molar eruption age of 6.02 years for M_1 and 11.31 years for M_2, and a 6.56-year subadult interval, with an average eruption age of 17.87 years for M_3. It is worth noting that molar eruption ages can vary significantly among populations, particularly for M_3. We adopted the age intervals indicated by Ash and Nelson (2003); if these ranges were to be smaller or greater, the computed wear rates would represent under- or overestimations of actual rates, respectively.

We also computed wear rates for an overall age interval from the eruption of M_1 (5.5 years) to an adult age (E_m years) at which M_1 and M_2 exhibit equal dentin exposure areas (the D value of M_2 matched that of M_1). This interval encompasses both the juvenile and subadult intervals, as well as an adult period whose length may vary depending on the variation of wear rates within the intervals. We did not compute a separate wear rate for the adult interval alone because some samples lacked M_3 teeth showing dentin exposure.

While molar eruption undeniably occurs earlier than the onset of dentin exposure, we use molar eruption ages to define the age intervals. Thus, the span between eruption and the onset of dentin exposure of one molar is included at the beginning of the age interval considered for computing wear rates. We assume that the interval between the eruptions of two consecutive molars does not differ significantly from the interval between the onsets of dentin exposure for those same molars if the wear rate remains consistent within the short span from eruption to dentin exposure onset. Lower molar crown formation, crown eruption, and root completion ages in modern humans support consistent age intervals for average developmental events of consecutive molars (Ash & Nelson, 2003).

For each age interval, using the intercept $\ln a$ for each molar in the regression models in Eq. (2), $\ln S = \ln a + b \ln D$, for each molar, we computed two dentin exposure rates.

$$r_i = \frac{\ln a_{i+1} - \ln a_i}{12\, t} \tag{5}$$

$$w_i = \frac{a_{i+1} - a_i}{t} \tag{6}$$

The r (Eq. (5)) wear rate value is a monthly (divided by 12) percent (%) rate (r) of dentin exposure for a given age interval in years (t). This equation derives from the *compound interest rate* function $S_{i+1} = S_i e^{12rt}$, where the overall dentin exposure at the end of the interval (S_{i+1}, accrued capital) is a function of the wear rate (r, interest rate), the elapsed time (t, duration of the investment in years), and the dentin exposure at the beginning of the interval (S_i, invested capital). The accrued dentin exposure is a function of time that depends on the rate of accumulation in the same way as invested capital. In contrast, the w (Eq. (6)) wear rate (mm^2/year) represents the yearly change in dentin exposure for the age intervals considered (juvenile, subadult, or otherwise). The values ln a and a are obtained from the Linear model ln S = ln $a + b$ ln D for each molar. Thus, r_1 and w_1 are wear rate measures for the juvenile interval, r_2 and w_2 refer to the subadult age interval, and r_m and w_m refer to the age interval from the eruption of M_1 to the adult E_m age at which M_1 and M_2 show the same D_m value of dentin exposure. To compute r_m and w_m, the D_m dentin exposure at age E_m is required and can be computed by equalizing the dependent variable (ln S) of the linear regression models (ln S = ln $a + b$ ln D) of two consecutive molars (ln S_{M1} = ln S_{M2}, Eq. 7). From this, we can compute the D_m value independently of the wear rates (Eq. (8)). The predicted age (E_m) at which M_1 and M_2 show the same dentin exposure areas (D_m) is used to define an adult age interval. This interval goes from ln S_{M3} to ln S_m (from age E_{M3} to E_m) (ln S_m = ln $a + b$ D_m), in the same way that the subadult interval goes from ln S_{M2} to ln S_{M3} (from age E_{M2} to E_{M3}), and the juvenile interval goes from ln S_{M1} to ln S_{M2} (from age E_{M1} to E_{M2}). For each age interval, the wear rates are expressed as a percentage (%) of dentin exposure per month (r) or in mm^2 per year (w), so the length of the interval is not relevant for comparative purposes.

$$\ln a_{M1} + b_{M1} \ln D_m = \ln a_{M2} + b_{M2} \ln D_m \tag{7}$$

$$D_m = e^{\frac{\ln a_{M1} - \ln a_{M2}}{b_{M2} - b_{M1}}} \tag{8}$$

For comparative purposes, we computed the same dentin exposure rates for the *Coimbra International Exchange Collection*, XVIII-XIX c. from Portugal (Cunha & Wasterlain, 2007).

Estimation of Age at Death

The estimation of the age at death of any individual derives from a regression model between eruption ages and the dentin exposure area of the first molar. We used the eruption ages (E_i) of all three molars (5.5 for M_1, 11.5 for M_2, and 18.5 for M_3) as the dependent variable and the corresponding dentin exposure areas of M_1 as the independent variable. The D_i values were computed from Eq. (1) as $D_i = \sqrt[b]{\frac{S_i}{a}}$. We tested three regression models (Linear, Power, and Compound) to predict age at death (E) from the variables D, ln D, S, and ln S for the M_1 to determine which model and variable better predicted the available skeletal age (A). Eventually, the linear model $E = c + b(aD^b)$ was adopted (Eq. (3)). The estimated ages (E) for all individuals were correlated with the physiological skeletal age (A) available for the combined Chinese sample. For such an estimation of age at death to be reliable, the predicted ages need to be not only highly correlated (association) but also very close to the actual ages (precision). The estimation of the precision of an age prediction was not the objective of the present research, since only rough age estimation ranges of skeletal age were available, rather than precise ages, nor to say actual ages.

Measurement Error and Statistical Analyses

A single observer (SY) made all the D measurements by manually outlining the dentin exposure patches on the occlusal molar crown surface. Measuring errors may arise either by erroneously defining the dentin patch boundaries or by under or over-representing dentin patches. For testing possible biases in dentin exposure characterization between observers, a second observer (APP) reanalyzed the complete Jiayi specimens, the largest and best-preserved sample. APP independently applied the specimen selection criteria and measured again the newly selected specimens from the Jiayi samples. We performed paired t-test for sample mean comparisons between observers and computed anew the same wear rates for the duplicated sample.

A t-test (Eq. (9)) was used to compare slope values (b_i, b_j) between two samples (n_i, n_j) for the linear regression models $\ln S = \ln a + b \ln D$.

$$t = \frac{b_i - b_j}{\sqrt{e_i^2 + e_j^2}};\ d.f. = ni + nj - 4. \tag{9}$$

We used SPSS v.27 (IBM, Armonk, NY, USA, licensed to UB) for all statistical analyses. The significance level was set to $\alpha = 0.05$.

Results

A sample of 328 lower molars showed dentin exposure (Table 1). However, the sample sizes by molar type decreased from M_1 to M_3 in all the groups considered (Table 2). Since the posterior molars erupt later than the preceding molars, not all analyzed quadrants showed dentin exposure on M_3 or M_2, significantly reducing their sample sizes. Banlashan and Dunping lacked M_3 molars with dentin exposure.

Table 2 Summary statistics of the dentin exposure area by site, tooth, and sex

		Female			Male			All		
		N	Mean	SD	*N*	Mean	SD	*N*	Mean	SD
Banlashan	M_1	10	20.11	19.42	7	39.63	31.82	17	28.15	26.27
	M_2	5	14.78	22.80	6	23.59	32.45	11	19.59	27.49
Dunping	M_1	8	21.81	16.92	8	21.88	20.92	16	21.84	18.38
	M_2	5	14.38	6.47	3	25.83	20.39	8	18.68	14.22
Houtaomuga	M_1	14	31.05	21.23	30	49.15	26.72	45	42.50	26.65
	M_2	9	22.02	23.10	27	33.25	27.49	36	30.44	26.60
	M_3	3	5.40	2.67	3	6.04	3.41	6	5.72	2.76
Jiayi	M_1	38	36.46	25.08	46	52.87	27.13	100	42.00	27.90
	M_2	27	23.93	24.42	36	32.95	24.18	69	29.23	24.54
	M_3	10	13.71	10.67	8	16.26	14.05	20	14.83	11.39

N sample size, *Mean* average dentin exposure area (D, in mm^2), *SD* standard deviation of D

Houtaomuga A only showed one M_3 molar with dentin exposure and Houtaomuga B had five. These small sample sizes for M_3 led us to treat Houtaomuga as a single sample. Dentin exposure areas decreased from front to back (M_1–M_3), reflecting the later eruption age of the posterior molars. Males showed somewhat higher average D values than females for the three molars in all the populations considered (Table 2). We did not attempt comparisons of dentin exposure areas among groups due to the significant dependence of dentin exposure on the age distributions within each group, which varied considerably across samples. Furthermore, the dentin exposure areas (D) did not follow a normal distribution (Kolmogorov−Smirnov test, K–S) for M_1 ($N = 178$, K–S = 0.135, $P < 0.001$) and M_2 ($N = 124$, K–S = 0.124, $P < 0.001$), whereas for M_3, the test was not significant ($N = 28$, K–S = 0.152, $P = 0.124$), likely due to its reduced sample.

Interobserver Measurement Error

Despite following the same sample selection criteria, the Jiayi sample selected by SY was larger ($N = 164$; 88 M_1, 59 M_2, 17 M_3) than that measured by APP ($N = 125$; 66 M_1, 40 M_2, 19 M_3) who discarded some cases for being damaged, heavily worn, or not showing clearly defined dentin exposure patches. All the *t*-test comparisons between observers, using paired measurements, were significant ($P < 0.001$). In all cases, SY showed larger dentin exposure measurements than APP by tooth type: M_1 ($N = 66$), $t = 6.167$, 12.7% difference between observers; M_2 ($N = 40$), $t = 3.255$, 16.5%; M_3 ($N = 19$), $t = 3.436$, 37.5%. Despite the differences in average D values being significant, the measurements by the two observers were highly correlated: $r = 0.983$ for M_1 ($F = 1795.370$, $P < 0.001$), $r = 0.965$ for M_2 ($F = 511.545$, $P < 0.001$), and $r = 0.777$ for M_3 ($F = 25.828$, $P < 0.001$). The parameters of the linear regression models of ln D over ln S ($\ln S = \ln a + b \ln D$) by tooth type showed similar ln a and b values in both observers (Table 3). The slopes (b) of the models did not significantly differ between observers ($P = 0.930$ for M_1, $P = 0.974$ for M_2, and $P = 0.954$ for M_3). The differences between the intercepts (ln a), a key factor for computing the wear rates, only differed between observers in 0.071 mm^2 for M_1, − 1.822 mm^2 for M_2, and 1.021 mm^2 for M_3. These differences resulted in dentin exposure rate divergences (Table 3) ranging from − 0.25 to 0.21%/month for the r_i values and from − 0.36 to 0.47 mm^2/year for the w_i values. All the dentin exposure rates computed for the age intervals considered were consistent in the two observers.

Dentin Exposure as a Wear Indicator

Overall trends of increasing dentin exposure (D) with wear score (WS) were observed in all molars for the combined sample (Fig. 3). However, when WS = 8, wear significantly impacted the molar root, and the dentin exposure area decreased. By tooth type (excluding the wear score value of 8), and for the entire sample, all three tested least square regression models between WS (independent variable) and D (dependent variable)—Linear, $D = b$ WS; Quadratic, $D = b\ \mathrm{WS} + b_1\ \mathrm{WS}^2$; and Power, $D = \mathrm{WS}^b$—showed high significance

Table 3 Comparison of dentin exposure parameters between independent observers (SY and APP indicated as subindices) by tooth type (M_1, M_2, M_3)

	M_1	M_2	M_3		APP	SY	Dif
ln a_{APP}	−0.108	2.852	3.942	r_1	4.11	4.36	−0.25
ln a_{SY}	−0.190	2.952	3.922	r_2	1.51	1.35	0.16
a_{APP}	0.898	17.322	51.522	r_3	5.62	5.71	−0.09
a_{SY}	0.827	19.144	50.501	r_m	1.23	1.02	0.21
b_{APP}	1.111	0.465	0.302	w_1	2.74	3.05	−0.31
b_{SY}	1.138	0.490	0.334	w_2	5.70	5.23	0.47
t-test	0.088	0.032	0.058	w_3	8.44	8.28	0.16
P	0.930	0.974	0.954	w_m	4.21	4.57	−0.36

ln a and *b* intercept and slope (respectively) of the regression model ln $S=b+\ln D$, *a* dentin exposure in mm^2 at the intercept, *t-test* parameter of the statistical test comparing the slopes of the two observers, *P* significance probability of the test (non-significant), r_1 wear rate (%/month) for the juvenile interval, r_2 wear rate (%/month) for the subadult interval, r_3 wear rate (%/month) for an adult interval from M_3 eruption to the E_m age (when M_1 and M_2 match their dentin-exposed surfaces), r_m wear rate (%/month) for the interval from the eruption of M_1 to the adult E_m age, w_1 wear rate (mm^2/year) for the juvenile interval, w_2 wear rate (mm^2/year) for the subadult interval, w_3 wear rate (mm^2/year) for an adult interval, w_m wear rate (mm^2/year) for the interval from the eruption of M_1 to the adult E_m age

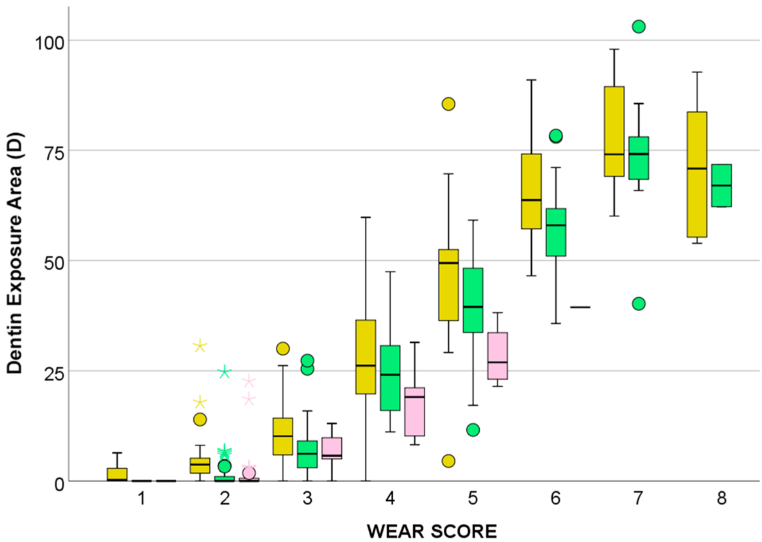

Fig. 3 Box plots of 3D dentin exposure areas categorized by wear score (from 1 to 8) and tooth type: M_1 (gold), M_2 (green), and M_3 (pink). Outliers are indicated by circles (95% confidence interval) or 5-point stars (99% confidence interval)

Table 4 Standardized least square regression models (Linear, Quadratic, Power)1 of the wear score (WS, independent variable) on the 3D dentin exposure (D, dependent variable)2 by site and tooth type

Site	Tooth	N	Model	R^2	e	F	P	b	b_1
Banlashan	M_1	17	Linear	0.866	14.316	103.579	< 0.001	8.676	1.813
			Quadratic	0.969	7.161	231.437	< 0.001	− 0.453	
			Power	0.985	0.382	1072.404	< 0.001	2.321	
	M_2	11	Linear	0.793	15.626	38.222	< 0.001	7.710	1.995
			Quadratic	0.964	6.860	120.599	< 0.001	− 2.416	
			Power	0.778	1.211	35.059	< 0.001	1.815	
Dunping	M_1	16	Linear	0.791	13.306	56.745	< 0.001	6.697	1.302
			Quadratic	0.828	12.479	33.785	< 0.001	1.000	
			Power	0.937	0.740	223.568	< 0.001	2.215	
	M_2	8	Linear	0.796	11.070	27.325	< 0.001	4.560	1.711
			Quadratic	0.889	8.819	24.041	< 0.001	− 3.654	
			Power	0.982	0.398	388.541	< 0.001	1.888	
Houtaomuga	M_1	44	Linear	0.894	16.458	361.762	< 0.001	9.375	1.852
			Quadratic	0.947	11.736	377.010	< 0.001	− 0.934	
			Power	0.989	0.385	3725.412	< 0.001	2.269	
	M_2	35	Linear	0.822	16.667	156.688	< 0.001	7.598	2.130
			Quadratic	0.936	10.161	240.012	< 0.001	− 3.738	
			Power	0.949	0.704	626.776	< 0.001	2.034	
	M_3	6	Linear	0.923	1.894	60.301	< 0.001	2.059	0.187
			Quadratic	0.927	2.070	25.336	0.005	1.468	
			Power	0.981	0.255	263.473	< 0.001	1.621	
Jiayi	M_1	97	Linear	0.915	14.457	1027.777	< 0.001	9.728	1.458
			Quadratic	0.951	11.010	921.239	< 0.001	1.599	
			Power	0.982	0.466	5320.577	< 0.001	2.303	
	M_2	69	Linear	0.861	14.281	421.953	< 0.001	8.053	1.750
			Quadratic	0.930	9.420	529.592	< 0.001	− 1.015	
			Power	0.941	0.818	907.205	< 0.001	2.129	
	M_3	20	Linear	0.805	8.401	78.256	< 0.001	4.710	1.019
			Quadratic	0.841	7.786	47.617	< 0.001	0.607	
			Power	0.844	1.018	102.994	< 0.001	1.923	
All	M_1	174	Linear	0.896	15.143	1491.552	< 0.001	9.376	1.627
			Quadratic	0.946	10.994	1493.100	< 0.001	0.484	
			Power	0.981	0.469	9040.788	< 0.001	2.289	
	M_2	123	Linear	0.832	15.249	604.281	< 0.001	7.653	1.909
			Quadratic	0.928	9.780	822.346	< 0.001	− 2.269	
			Power	0.931	0.811	1563.317	< 0.001	2.062	
	M_3	26	Linear	0.767	8.140	82.140	< 0.001	4.259	1.175
			Quadratic	0.824	7.212	56.232	< 0.001	− 0.298	
			Power	0.857	0.906	150.438	< 0.001	1.868	

R^2 coefficient of determination, e standard error of the estimation, F statistic for the regression model, P probability of significance, b slope of the standardized regression models

[1]Linear, $D = b\text{WS}$; Quadratic, $D = b\text{WS} + b_1\text{WS}^2$, Power:$D = \text{WS}^b$

[2]Smith's (1984) score of 8 and the teeth lacking dentin exposure ($D=0$) were not considered for the regressions. The models with the highest R^2 and F values within each tooth are shown in bold

($P < 0.001$) (Table 4). The Linear model consistently exhibited the lowest performance, displaying a large dispersion of data (mean error), although still statistically significant. This implies that a nonlinear model might provide a better prediction of D from WS. The nonlinear regressions by samples largely overlapped for M_1 (Fig. 4A). However, for M_2, the Dunping sample ($N = 8$) displayed a somewhat flatter curve (Fig. 4B). Regarding M_3, only Jiayi ($N = 20$) and Houtaomuga ($N = 6$) data could be plotted (Fig. 4C). The Power function exhibited the smallest standard error of the estimation (e) and explained the highest percentage of the total variance (R^2, coefficient of determination) in all samples except for the M_2 of Banlashan (Table 4). Despite the macroscopic scoring of wear being a standard bio-archaeological practice, discrete wear scores appear to artificially compress a wide range of variability in a continuous measure of dentin exposure.

Dentin Exposure as an Age Estimator

The actual ages at death of the studied individuals were unknown. However, archaeologically estimated ages derived from skeletal markers enabled the testing of the hypothesis of a nonlinear relationship of the variable D over time. Since the bio-archaeological estimations of age at death provided age ranges instead of precise ages, for simplification of this analysis, we used the midpoint of the estimated age interval for each individual as a rough measure of skeletal age, rather than the actual, unknown age at death. Nevertheless, D increased in all molars as individuals aged and exhibited a significant correlation ($P < 0.001$) with both wear scores ($r = 0.907$ for M_1, $r = 0.914$ for M_2, and $r = 0.778$ for M_3) and archaeologically estimated ages ($r = 0.623$ for M_1, $r = 0.431$ for M_2, and $r = 0.002$ for M_3, $P = 0.992$); this last correlation was not significant for M_3.

Both the Compound ($D = a\ b^{\mathrm{Age}}$) and the Power ($D = a\ \mathrm{Age}^b$) regression models between D and Age were highly significant (Table 5) using the Linear models derived from the ln-transformed variables. Overall, the Compound models ($\ln D = \ln a + \mathrm{Age} \ln b$) showed larger R^2 values (75.2–98.9%) than the Power ones ($\ln D = \ln a + b \ln \mathrm{Age}$) (48.2–96.5%). The Compound model explained a larger percentage of the total variance than the Power model for most analyses (6 of the 10 tests made), except for Dunping M_2, Houtaomuga M_1 and M_3, and Jiayi M_3. For the complete joint sample, the Compound model performed better for M_1 ($N = 165$) and M_2 ($N = 113$), while the Power model performed somewhat better for M_3 ($N = 23$). The Linear model ($D = a + b$ Age, not shown in Table 5) always performed the least in all groups, suggesting that a nonlinear model better explained the relationship between age and dentin exposure.

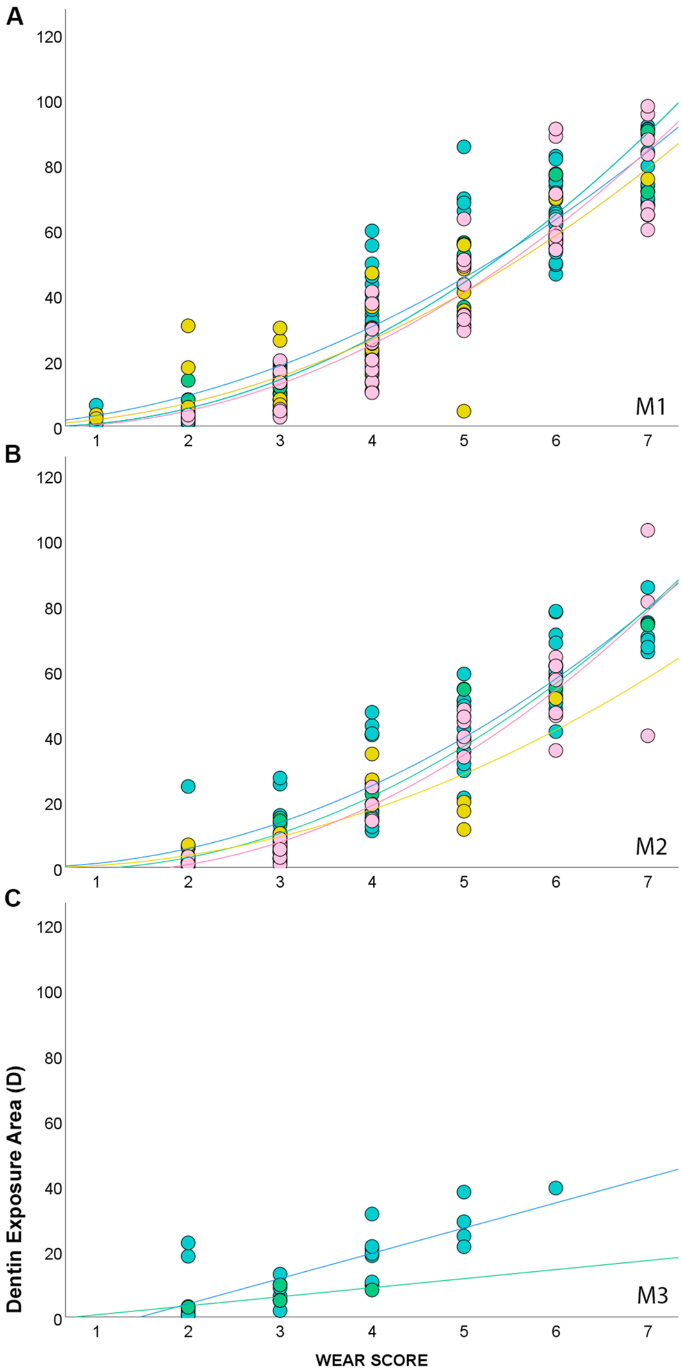

Fig. 4 Plots of dentin exposure areas (mm^2) (Y-axis) by wear scores (from 1 to 7, X-axis) across sites (Banlashan in green, Dunping in gold, Houtaomuga in pink, Jiayi in blue), and tooth type (**A** M_1, **B** M_2, **C** M_3). Exponential regression lines are displayed for each site. Wear score 8 was excluded as it pertains to the root of the molar teeth after the complete wear of the crown. M_3 data were unavailable for Dunping and Houtaomuga

Table 5 Standardized least square regression models (Compound, Power)[1] of the skeletal age (Age, independent variable) on the 3D dentin exposure area (*D*, dependent variable), by site and tooth

Site	Tooth	*N*	Model	R^2	*e*	*F*	*P*	*b*
Banlashan	M_1	17	**Compound**	0.978	0.469	707.430	< 0.001	1.097
			Power	0.932	0.820	220.217	< 0.001	0.855
	M_2	11	**Compound**	0.567	1.691	13.106	0.005	1.053
			Power	0.482	1.850	9.318	0.012	0.481
Dunping	M_1	16	**Compound**	0.932	0.772	204.207	< 0.001	1.090
			Power	0.914	0.866	158.935	< 0.001	0.803
	M_2	8	Compound	0.958	0.615	158.596	< 0.001	1.078
			Power	0.965	0.555	195.821	< 0.001	0.773
Houtaomuga	M_1	44	Compound	0.959	0.732	1002.728	< 0.001	1.139
			Power	0.962	0.701	1097.214	< 0.001	1.085
	M_2	35	**Compound**	0.848	1.212	188.989	< 0.001	1.102
			Power	0.838	1.249	176.135	< 0.001	0.840
	M_3	6	Compound	0.881	0.645	36.842	0.002	1.057
			Power	0.925	0.512	61.489	< 0.001	0.492
Jiayi	M_1	88	**Compound**	0.953	0.744	1765.687	< 0.001	1.119
			Power	0.939	0.848	1339.230	< 0.001	1.002
	M_2	59	**Compound**	0.818	1.313	260.244	< 0.001	1.087
			Power	0.780	1.444	205.292	< 0.001	0.780
	M_3	17	Compound	0.673	1.513	32.873	< 0.001	1.062
			Power	0.701	1.447	37.477	< 0.001	0.608
China (all)	M_1	165	**Compound**	0.940	0.826	2583.000	< 0.001	1.117
			Power	0.936	0.856	2396.850	< 0.001	0.996
	M_2	113	**Compound**	0.800	1.341	446.759	< 0.001	1.086
			Power	0.777	1.413	390.971	< 0.001	0.766
	M_3	23	Compound	0.700	1.328	51.321	< 0.001	1.061
			Power	0.726	1.270	58.204	< 0.001	0.581

The models with the highest R^2 and *F* values within each tooth are shown in bold

R^2 coefficient of determination, *e* standard error of the estimation, *F* statistic for the regression model, *P* probability of significance, *b* slope of the standardized regression models

[1]Compound, $D = b^{Age}$; Power, $D = Age^b$

Group Comparisons Using the Power Function

The Linear regression models $\ln S = \ln a + b \ln D$ (derived from the Power model) showed highly significant ($P < 0.005$) R^2 values (ranging from 0.720 to 0.984) for all the molars and samples (Table 6), except for Houtaomuga M_3 ($N = 6$, $R^2 = 0.004$, $P = 0.910$) and for the Coimbra comparative sample M_3 ($N = 6$, $R^2 = 0.631$, $P = 0.059$). These results are indicative that *D* is a reliable predictor of *S* provided the sample sizes for each molar are large enough.

The slopes (*b*) of the linear model for M_1 were significantly larger than one ($P < 0.001$) in all four Chinese samples (Table 7), ranging from 1.167 to 1.198.

Table 6 Linear least square regression models between ln *S* (dependent variable) and ln *D* (independent variable) by site and tooth type (ln $S = \ln a + b \ln D$)

		N	***r***	R^2	***e***	***F***	***P***
Banlashan	M_1	17	0.992	0.984	0.154	909.6	< 0.001
	M_2	11	0.849	0.720	0.534	23.2	< 0.001
Dunping	M_1	16	0.987	0.973	0.196	508.7	< 0.001
	M_2	8	0.915	0.836	0.258	30.7	0.001
Houtaomuga	M_1	44	0.987	0.973	0.182	1535.6	< 0.001
	M_2	35	0.925	0.856	0.256	195.7	< 0.001
	M_3	6	0.060	0.004	0.584	0.014	0.910*
Jiayi	M_1	97	0.985	0.971	0.219	3174.2	< 0.001
	M_2	69	0.892	0.795	0.341	260.2	< 0.001
	M_3	20	0.857	0.734	0.280	49.7	< 0.001
China (all)	M_1	174	0.987	0.974	0.201	6350.0	< 0.001
	M_2	123	0.885	0.784	0.350	438.0	< 0.001
	M_3	26	0.758	0.575	0.365	32.5	< 0.001
Coimbra[1] (Portugal)	M_1	123	0.977	0.955	0.262	2586.0	< 0.001
	M_2	37	0.717	0.514	0.754	37.0	< 0.001
	M_3	6	0.795	0.631	0.550	6.9	0.059*

N sample size, *r* Pearson's correlation coefficient, R^2 coefficient of determination, *e* standard error of the regression model, *F* statistic for the regression, *P* significance probability of the regression model

*Non-significant *P* values

[1]Coimbra International Exchange collection, Coimbra (Portugal)

These slopes did not differ significantly among the samples (*t*-test, *P* ranging from 0.399 to 0.899). The slopes of the linear models varied greatly for M_2, with the Dunping sample showing the highest value ($b = 0.812$), significantly differing from the other three samples (Table 7): Banlashan ($b = 0.425$, $P = 0.039$), Jiayi ($b = 0.454$, $P = 0.019$), and Houtaomuga ($b = 0.470$, $P = 0.029$). The slopes for these three samples did not differ significantly from each other ($P = 0.636$ for the Banlashan-Houtaomuga comparison, $P = 0.717$ for Houtaomuga-Jiayi, and $P = 0.757$ for Banlashan-Jiayi).

The regression models by tooth type and site for the ln-transformed variables showed a strong relationship between the intercepts (ln *a*) and the slopes (*b*). The M_1 teeth had the largest slopes and the smallest intercepts, the M_2 teeth had intermediate slope and intercept values, and the M_3 teeth had the largest intercepts and the lowest slopes. For M_2, the Dunping sample showed distinct values for *b* and ln *a* (Table 7). This overall trend is consistent with the greater intercept values and smaller slopes of later erupting molars.

For the joint sample (Table 7, Fig. 5 top left), M_1 showed the largest slope ($b = 1.173$) and the smallest intercept ($\ln a = -0.296$), followed by M_2 ($b = 0.458$, $\ln a = 2.950$), and then M_3 ($b = 0.337$, $\ln a = 3.876$). Consequently, the three regression lines tended to converge to a point where all molars would show the same *D* values. This indicates that the three molars do not expose their dentin at the same

Table 7 Linear least square regression models between ln S (dependent variable) and ln D (independent variable) by site and tooth type ($\ln S = \ln a + b \ln D$)

Genus		*ln a*	t_i	P_i	b	e_s	t_s	P_s
Banlashan	M_1	-0.357	-3.0	0.009	1.181	0.039	30.2	<0.001
	M_2	2.994	13.8	<0.001	0.425	0.088	4.8	<0.001
Dunping	M_1	-0.215	-1.5	0.166*	1.160	0.051	22.6	<0.001
	M_2	1.609	3.9	0.008	0.812	0.147	5.5	0.001
Houtaomuga	M_1	-0.365	-3.4	0.002	1.198	0.031	39.2	<0.001
	M_2	2.874	28.0	<0.001	0.470	0.034	14.0	<0.001
	M_3	4.115	4.5	0.011	0.064	0.536	0.12	0.910*
Jiayi	M_1	-0.284	-3.9	<0.001	1.167	0.021	56.3	<0.001
	M_2	3.026	35.0	<0.001	0.454	0.028	16.1	<0.001
	M_3	3.956	33.7	<0.001	0.329	0.047	7.1	<0.001
China (all)	M_1	-0.296	-5.9	<0.001	1.173	0.015	79.7	<0.001
	M_2	2.950	44.9	<0.001	0.458	0.022	20.9	<0.001
	M_3	3.876	27.8	<0.001	0.337	0.059	5.7	<0.001
Coimbra[1] (Portugal)	M_1	0.080	2.3	0.024	1.027	0.020	50.6	<0.001
	M_2	1.792	11.4	<0.001	0.735	0.121	6.1	<0.001
	M_3	2.545	8.6	0.001	0.657	0.251	2.6	0.059*

ln a intercept of the linear model for $\ln D = 0$, t_i Student's t statistic for the null hypothesis $\ln a = 0$, P_i significance probability for the null hypothesis $\ln a = 0$, b slope of the regression model, e_s standard error of the slope, t_s Student's t statistic for the null hypothesis $b = 0$, P_s significance probability for the slope

*Non-significant P values

[1]Coimbra International Exchange collection, Coimbra (Portugal)

rates; overall, M_3 wears at a faster, non-constant rate compared to M_2, and M_2 wears faster than M_1. This overall pattern was observed in all the samples considered. The regression slopes and intercepts for M_1 were almost identical across all four skeletal collections (Table 7, Fig. 5 top right). For M_2, however, the Dunping sample showed a significantly larger slope and a smaller intercept compared to the other sites (Table 7, Fig. 5 bottom left). Sample sizes for M3 were too small for population comparisons (Table 7, Fig. 5 bottom right). Assuming identical dentin exposure onset ages in all four Chinese samples, Dunping exhibited less dentin exposure at the eruption of M_2 than the other samples, indicating reduced wear rates for this sample. The combined sample of all Chinese specimens showed an ln a value of 2.950, equivalent to $a = 19.1$ mm^2 of dentin exposure for M_1 at the onset of dentin exposure for M_2. These values were 2.994 (20.0 mm^2) for Banlashan, 2.874 (17.7 mm^2) for Houtaomuga, and 3.026 (20.6 mm^2) for Jiayi, while Dunping showed a reduced intercept value of 1.609 (5.0 mm^2) (Table 7).

Wear Rates Within Age Intervals

Overall wear rates were higher in the juvenile interval ($r_1 = 4.51$%/month and $w_1 = 0.834$ mm^2/year) than in the subadult interval ($r_2 = 1.29$%/month and $w_2 = 0.420$

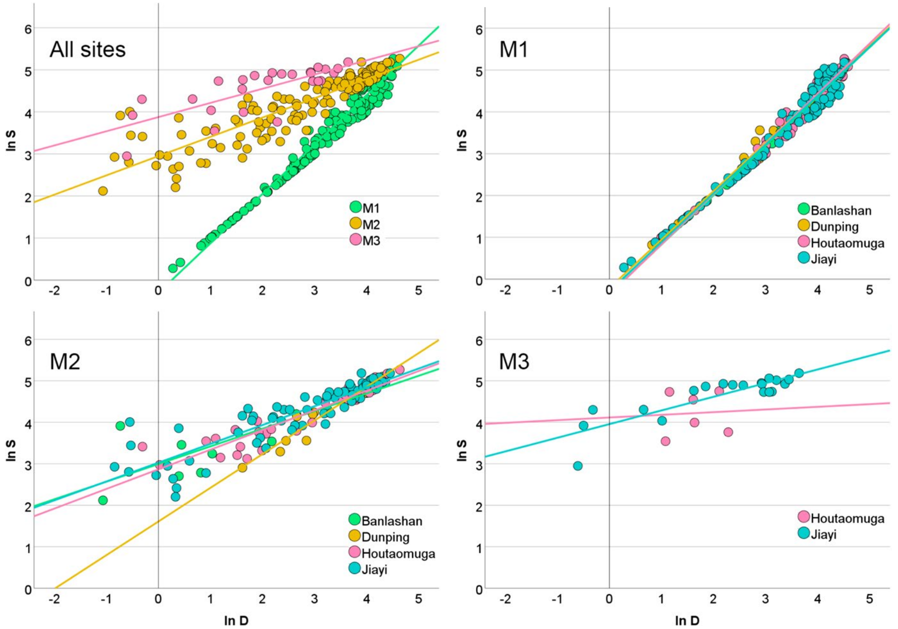

Fig. 5 Contribution of dentin exposure (ln D, X-axis) to cumulative dentin exposure (ln S, Y-axis) by molar type (M_1, M_2, M_3) and sites; intercepts with the vertical axis (ln a) for ln $D=0$ ($D=1$ mm^2) are indicated. Top left: joint sites by tooth type (M_1 green, M_2 gold, M_3 pink); top right: M_1 by site (Banlashan green, Dunping gold, Houtaomuga pink, Jiayi blue); bottom left: M_2 by site; bottom right: M_3 by site

Table 8 Wear rate estimations r (%/month) and w (mm^2/year) derived from the linear regression model $E=c+pD$ using the data in Table 7. r_1 and w_1 show the dentin exposure rates for the 6-year interval from 5.5 to 11.5 years (juvenile interval); r_2 and w_2 show the dentin exposure rates for the 7-year interval from 11.5 to 18.5 years (subadult interval); r_m and w_m show the dentin exposure rates for the interval from 5.5 years to the E_m adult age; D_m is the dentin exposure of M_1 and M_2 at age E_m; E_m is the age at which D is equal in M_1 and M_2; S_m is the predicted S value at age E_m; c is the intercept and p is the slope of the regression model $E=c+pD_{M1}$

	r_1	r_2	r_m	w_1	w_2	w_m	D_m	E_m	S_m	c	p
Banlashan	4.65	–	1.41	3.21	–	4.21	84.14	36.51	131.35	5.127	0.373
Dunping	2.53	–	0.17	0.70	–	1.19	188.93	300.93	352.48	3.928	1.572
Houtaomuga	4.50	1.48	1.66	2.84	6.22	5.34	85.56	32.22	143.32	5.869	0.308
Jiayi	4.60	1.11	1.24	3.31	4.52	4.65	103.79	41.81	169.63	5.273	0.352
China (all)	4.51	1.10	1.25	3.06	4.16	4.29	93.68	40.92	152.82	5.233	0.381
Coimbra[1]	2.38	0.90	0.33	0.82	0.96	2.89	351.78	82.71	446.44	5.714	0.438

[1]Coimbra International Exchange Collection, XVIII-XIX c., Coimbra (Portugal)

mm^2/year), indicating that M_1 wore fast when it was the only molar involved in food processing. After the eruption of M_2, the overall rates of dentin exposure decrease in the subadult interval. Houtaomuga and Jiayi exhibited this same trend and similar wear rates for both periods. Banlashan and Dunping had no third molars with dentin exposure, so we computed wear rates only for the juvenile period (Table 8). Banlashan showed wear rates similar to those of Houtaomuga and Jiayi, whereas Dunping showed smaller wear rates ($r_1 = 2.53\%$/month and $w_1 = 0.240$ mm^2/year). The reduced wear rates in Dunping resulted in an increased D_m value (188.93 mm^2) at age E_m compared to the other samples (Table 8). With smaller wear rates, M_1 and M_2 require a longer time to reach the same D_m value, consequently resulting in greater dentin exposure areas at age E_m. The E_m age for Dumping was 300.93 years, clearly beyond life expectancy (which indicates reduced wear rates for this sample), followed by Jiayi (41.81 years), Banlashan (36.51 years), and Houtaomuga (32.22 years). The comparative Coimbra sample showed an E_m age of 82.71 years, indicating smaller wear rates than the Chinese samples except for Dunping.

Dentin Exposure and Age-at-Death Estimation

The estimation of age at death (E) for the combined Chinese sample required prior knowledge of how to predict E from D (Eq. (3)). The three regression models tested (Linear, Power, Compound) used the molar eruption ages (E) as the dependent variable (5.5 years for M_1, 11.5 years for M_2, and 18.5 years for M_3). As the independent variable, we used the dentin exposure area (D, in mm^2) to predict age (E). The D values were computed using Eq. (4): D was 1.00 mm^2 for M_1, 15.92 mm^2 for M_2, and 35.05 mm^2 for M_3. Only the Linear model ($E = c + pD$) for the non-ln-transformed E and D variables yielded a statistically significant regression for predicting age at death from the dentin exposure of M_1 ($p = 0.381$, $c = 5.233$; $R^2 = 0.999$, $F = 1370.5$, $P = 0.017$; $E = 5.233 + 0.381D$). We used this model to estimate the E_m age at which both the M_1 and M_2 teeth showed the same D_m value (obtained from Eq. (8)). Thus, the equation $E_m = 5.233 + 0.381D_m$ predicted an E_m value of 40.92 years to reach a D_m dentin exposure value of 93.68 mm^2 of dentin exposure in the whole Chinese sample. By population (Table 8), the E_m ages were 36.51 years ($D_m = 84.14$ mm^2) for Banlashan, 32.22 years ($D_m = 85.56$ mm^2) for Houtaomuga, and 41.81 years ($D_m = 103.79$ mm^2) for Jiayi, all three samples closely resembling each other. However, Dunping showed an E_m age of 300.93 years ($D_m = 188.93$ mm^2), a value beyond life expectancy, indicating that Dunping exhibited the smallest dentin exposure rates.

The overall r_m and w_m wear rates, encompassing all age periods (juvenile, subadult, and adult until the E_m age), were 1.25%/month and 4.16 mm^2/year, respectively. However, these values for Dunping were considerably smaller, 0.17%/month and 1.19 mm^2/year, respectively, clearly deviating from the other samples (Table 8). The contemporaneous, European sample from Coimbra showed a w_m of 2.89 mm^2/year, a value 46% smaller than that observed for Houtaomuga (Table 8). The average E_m age at which M_1 and M_2 showed the same dentin exposure was 82.71 years for Coimbra, a much larger value than for the combined Chinese sample (40.92 years). As expected, for smaller wear rates, higher ages at which the two molars would match their dentin exposure areas are observed.

Discussion

Several significant results are drawn from the present research. Firstly, we demonstrate that molar dentin exposure throughout life follows a distinct statistical model. While various regression functions were significant, the Power function provided the smallest least square deviations, with the advantage that linear equations can be derived by applying a logarithmic transformation of the D and S data. Secondly, we show that the slopes of the regression models differed among the lower molars analyzed within a tooth quadrant, indicating that dentin exposure rates differ in molar teeth, with M_1 exhibiting the smallest rate and M_3 the largest. Finally, we suggest that differences in the intercept and slope values of the regression models, and in the derived wear rates, are indicative of activity patterns related to food abrasives, chewing forces, and masticatory biomechanics. The proxy proposed for analyzing wear rates has the advantage of dealing with a continuous variable, rather than discrete scores of dentin exposure. We measure 3D dentin exposure surfaces because dentin wears down in a third dimension (dentin wears faster than enamel) that a 2D measure does not consider. A 3D scanning equipment, increasingly affordable, provides easy-to-implement and fast tools for making a 3D measure of dentin exposure surfaces by defining the dentin patch perimeter in the same way as for obtaining a 2D measure.

Wear Rate Differences Among Population

Our analysis of populations from various cemeteries spanning extensive geographical regions and representing different time periods, distinct climatic conditions, resource availability, and food processing techniques yielded significant results. We observed high dentin exposure rates, which were overall similar despite their heterogeneity (with a w_m wear rate of 4.21 mm^2/year in Banlashan, 4.65 in Jiayi, and 5.34 in Houtaomuga). This homogeneity is consistent with the consumption of hard and tough diets in most samples, likely including extrinsic abrasives incorporated into foodstuffs during food processing. The combination of cold, arid, and dry environmental conditions is likely the primary cause of the high wear rates observed in these Chinese samples. However, the Dunping site, whose inhabitants occupied much more diverse habitats, clearly differed from the other sites, showing wear rates in line with the Coimbra sample. The methodological approach used distinguished Dunping from the other sites, revealing a significantly higher slope for the linear regression model for M_2. This finding is consistent with the warmer, less arid, although more diverse, habitats and ecological conditions reported for Dunping inhabitants, who occupied an array of ecosystems ranging from forested to grassland and desert environments. The diet of the nomadic population from Dunping, a Bronze to Early Iron Age site, might have been less abrasive compared to that of the other samples, including the earlier Neolithic samples (Banlashan, Houtaomuga A) and the contemporaneous Bronze to Early Iron Age samples (Jiayi, Houtaomuga B). However, no comparisons between Houtaomuga A and B could be made. The Houtaomuga sample exhibited the highest dentin exposure rates and E_m age, despite their linear regression slopes for M_2 did not differ significantly from the other Chinese samples. This observation is consistent with the broad environmental conditions reported for this site.

As designed, the 3D dentin exposure areas of molar teeth proved to be a good proxy for characterizing molar wear rates, allowing for interpopulation comparisons. The wear rate calculations proposed depend only on the knowledge of the length of equivalent age intervals for the compared samples. This new methodological approach to dentin exposure characterization, designed here for the Chinese samples, shows that the overall 3D dentin exposure area (*S*) is a Power function of molar dentin exposure (*D*). Dentin exposure of the three molars (*S*) increases as the molars erupt and come to full functional occlusion, thus contributing to molar crown wear. The observed trends in the three molars matching their dentin exposure areas support the hypothesis that the posterior molars wear faster than the preceding molars, at least for the studied modern human samples.

Although the first molar contributes the most to the overall dentin exposure, as it erupts earlier than the other molars, dentin exposure rates are necessarily faster in the rearmost molars, as suggested by the fact that their dentin exposure surfaces eventually match that of the first molar. The second molar wears faster than the first one, and the third one wears even faster than the second one, as their regression functions also eventually intersect. Greater enamel thickness within molars may provide greater resistance to wear (Macho & Spears, 1999). Grine (2002, 2005) found that enamel thickness increases along the molar row in modern human molars but did not detect significant differences among permanent molars. Smith et al. (2006) found that upper molars showed significantly greater average enamel thickness than lower ones and that average enamel thickness increased significantly from M_1 to M_3 in both molar rows. Thus, the distal change in enamel thickness might be functionally related to higher bite forces exerted distally along the tooth row. Mahoney (2013) showed that, for the decidual dentition, thicker enamel on molars where bite forces are greater, combined with a reduced proportion of dentin, should facilitate the highest bite forces along the tooth row, independently of crow size. Our research shows that the thicker enamel and reduced size of the posterior lower molars have not fully compensated for the greater bite loadings on the posterior dentitions. Thus, dentin exposure rates remain faster on the posterior lower molars compared to the anterior ones.

Dietary Interpretations

The new proxy described here is a promising approach for between-group comparisons of dentin exposure rates to characterize overall dietary habits or ecological conditions. However, researchers must meet some methodological requirements: the three molars in a tooth row need to be characterized (either for being present or not yet erupted), and only molars showing dentin exposure can be considered. Samples are frequently scarce or poorly preserved, and fragmentation by tooth type quickly reduces sample sizes, especially for the third molar when wear rates are small. Our initial available sample of 528 skeletons ultimately resulted in a sample of 26 M_3

teeth (20 from Jiayi and 6 from Houtaomuga). The other two sites, Banlashan and Dunping, lacked M_3 teeth either because they had not yet erupted, showed no dentin exposure, were damaged, or were lost *postmortem*. Short life expectancies and reduced wear rates, common in modern humans, cause M_3 to rarely show dentin exposure before death, as seen in the Coimbra sample. Despite these difficulties, the 3D dentin exposure proxy proves to be consistent and reliable for comparing wear rates among populations with distinct socioeconomic practices or varying dietary habits. The Chinese samples studied showed striking similarities in their molar wear rate patterns, with the exception of Dunping. This consistency is indicative of highly abrasive diets under harsh environmental conditions, unrelated to their distinct socioeconomic lifestyles—whether hunter-gatherers, agriculturalists, or nomadic pastoralists with a shift to a greater focus on secondary animal products. Despite there seeming to be no clear association between dentin exposure rates and site-specific lifestyles and economies, similarities in food processing across populations might explain the resemblances. Practices such as grinding or otherwise processing millet grain, or using certain cooking technologies, could swamp signatures related to different types of diets. Despite archaeological reconstruction revealing few food processing artifacts in the sites studied, the nomadic populations might have used small millstones seasonally. Communalities in foodstuffs consumed and food preparation technology might have a greater effect on dentin exposure than the type of subsistence strategy. This conclusion requires confirmation with larger and more dietary distinct populations.

Future research on the proposed methodology for characterizing dentin exposure rates on molar teeth should focus on intra- and interpopulation comparisons among hunter-gatherer, agriculturalist, and pastoralist modern human populations. This will test whether socioeconomic strategies and diets can be discriminated against by measuring 3D dentin exposure rates of molar teeth, thereby determining if distinct sociocultural practices can be identified using wear rates. Research also needs to demonstrate that dentin exposure models are independent of the age distribution within the available samples, ensuring that sample sizes remain representative. Additionally, studies should focus on non-human species with varying life expectancies to determine which statistical model better explains dentin exposure with age.

Estimation of Age at Death

Finally, the dentin exposure models designed here might also contribute to resolving the challenges associated with estimating the physiological age at death of isolated archaeological or paleontological specimens. A biological estimation of age, reflecting physiological factors affecting skeletal markers, may not strongly correlate with the actual chronological ages of an individual. Dentin exposure serves as a physiological, diet-related indicator of age rather than an exact predictor of age. However, the 3D dentin exposure approach offers a statistical model for age prediction that, while dependent on both diet and physiological constraints, could provide an age-dependent sequence of archaeological remains. This could be particularly valuable for specimens of unknown ages at death.

Skeletal samples from primate populations, including humans, with known ages are scarce. Comparisons between actual ages at death and age predictions based on dentin exposure are necessary to validate this proxy as a reliable age indicator. We anticipate that the correlation between dentin exposure-based ages and actual ages would be significant, but the precision of age predictions—measured by the distance between actual and predicted ages—would vary depending on the statistical model used and the strength of the relationship between physiological age and chronological age. Precision in age estimations also depends on factors such as sample heterogeneity, underscoring the need to segment samples based on relevant criteria.

Conclusions

The 3D dentin exposure area of each lower molar tooth in various modern human archaeological samples shows a significant association with the overall dentin exposure in the respective quadrant. This correlation allows for determining the intercept value of regression models as an indicator of molar dentin exposure onset ages. These findings help predict dentin exposure rates across age intervals, identify the age at which two molars reach similar dentin exposure areas, and estimate age at death using model-based approaches. The study reveals dentin exposure as a nonlinear, age-dependent process, shedding light on ecological conditions and dietary habits among the studied populations. Specifically, Chinese populations from Banlashan, Houtaomuga, and Jiayi exhibit high molar dentin exposure rates indicative of their environmental conditions. In contrast, the Dunping site sample shows significantly lower wear rates across all molars, consistent with their highly diverse ecological habitats.

Supplementary Information The online version contains supplementary material available at https://doi.org/10.1007/s10816-024-09664-7.

Acknowledgements The authors want to thank Mr. Ruilin Mao (Gansu Institute of Cultural Relics and Archaeology), Dr. Zenglong Xiong (Jinan University), Mr. Long Wang (Academy of Turfanology), and Dr. Lixin Wang (Jilin University) for providing the materials for this study.

Author Contribution S.Y. and J.G. studied the skeletal collections in China, and S.Y. made the dental molds and measured the scans. L.M. and A.R. contributed to the development of the methodological procedures. A.E.D. helped with the molding and scanning procedures. Q.Z. and A.P-P. funded the project. A.P-P. designed the research and made the interobserver error analyses. S.Y. wrote the initial draft, and A.P-P. wrote the paper. S.Y., L.M., and A.R. greatly contributed to the final manuscript. All authors reviewed the manuscript.

Funding Open Access funding provided thanks to the CRUE-CSIC agreement with Springer Nature. This research was supported by the Chinese Fundamental Research Funds for the Central Universities [Projects:*On the origins of Chinese civilization, No. 2020YFC1521607, and Migration, Cultural Integration and Environmental Adaptation of Ancient Populations along the Belt and Road Based on the Bio-archaeological Perspective, No. 2022CXTD17]; theGraduate Innovation Fund of Jilin University and China Scholarship Council Grant[fellowship 2022134 to SY]; theBio-archaeological Study on Human Skeletons Unearthed from Dunping Cemetery in Zhang County, Gansu Province[23XWB046]; and the SpanishMinisterio de Ciencia e Innovación(MCIN) and ERDFA way of making EuropeEU [PID2020-112963GGB-I00 grant to APP, Ref. MCIN/AEI/10.13039/501100011033], as well as theMargarita Salaspostdoctoral contract, funded by the SpanishMinisterio de Universidades,a Next GenerationEU grant to SC.*

Data Availability Raw data is provided in the supplementary information file.

Declarations

Competing Interests The authors declare no competing interests.

References

Ash, M., & Nelson S. (2003). *Wheele's dental anatomy, physiology and occlusion*. Sounders Ed.

Benazzi, S., Bonetti, C., Cilli, E., & Gruppioni, G. (2008). Molar crown height: Not always a reliable method for the evaluation of age-at-death. *Journal of Archaeological Science, 35*(8), 2371–2378. https://doi.org/10.1016/j.jas.2008.03.005

Broca, P. (1879). Instructions relatives à l'étude anthropologique du système dentaire. *Bulletins de la Société d'anthropologie de Paris*, III° Série. *Tome, 2*, 128–163. https://doi.org/10.3406/bmsap.1879.5212

Brothwell, D. R. (1963). *Digging up bones. British Museum Natural History, London*. Oxford University Press.

Buikstra, J. E., & Ubelaker, D. H. (1994). Standards for data collection from human skeletal remains. *Arkansas Archaeological Survey Research Series* N. 44, Arkansas.

Chen, J. (2014). *A research on faunal remains excavated from Haminmangha site in Inner Mongolia and related problem study*. Master dissertation, Jilin University, Changchun. https://kns.cnki.net/KCMS/detail/detail.aspx?dbname=CMFD201402&filename=1014212419.nh. Accessed 13 June 2024

Chen, H., & Rong, W.S. (1998). The linear enamel hypoplasia of deciduous tooth. *Journal of Prevention and Treatment for Stomatological Diseases*, *3*, 59–60. https://kns.cnki.net/kcms2/article/abstract?v=VtJuiS_38noNIBZhMr5cvrCzj8HzbMKBwah8JA9nRVJtIseaTZIgLzksfT0PqC_CTvh_FqDAxlAedfGCYfDCEp5gbzaGJiDDNmOEycK-dNM-3V9nf0BOXQ==&uniplatform=NZKPT&language=CHS

Cheng, J., Zan, L., & Zhang, X. W. (2006). The Holocene vegetation and climate changes in the Turpan Basin of Xinjiang, China. In W. Dong (Ed.), *Proceeding of the Tenth Annual Meeting of the Chinese Society of Vertebrate Paleontology* (pp. 283–294). China Ocean Press.

Clement, A., & Hillson, S. (2012). Intrapopulation variation in macro tooth wear patterns – A case study from Igloolik, Canada. *American Journal of Physical Anthropology, 149*, 517–524. https://doi.org/10.1002/ajpa.22153

Cuesta-Torralvo, E., Pacheco, D., Martínez, L. M., Romero, A., Umbelino, C., Avià, Y., & Pérez-Pérez, A. (2021). Three-dimensional proxies to dental wear characterization in a known age-at-death skeletal collection. *Journal of Archaeological Method & Theory, 28*(4), 1261–1275. https://doi.org/10.1007/s10816-020-09496-1

Cunha, E., & Wasterlain, S. (2007). The Coimbra identified osteological collections. In G. Grupe & J. Peters (Eds.), *Skeletal series and their socio-economic context* (pp. 23–33). Verlag Marie Leidorf GmbH, Rahden/Westf.

Deter, C. (2009). Gradients of occlusal wear in hunter-gatherers and agriculturalists. *American Journal of Physical Anthropology, 138*, 247–254. https://doi.org/10.1002/ajpa.20922

Galbany, J., Estebaranz, F., Martínez, L. M., Romero, A., De Juan, J., Turbón, D., & Pérez-Pérez, A. (2006). Comparative analysis of dental enamel polyvinysiloxane impression and polyurethane casting methods for SEM research. *Microscopy Research Techniques, 69*(4), 246–252. https://doi.org/10.1001/jemt.20296

Gao, Y. (2021). *Cultural evolution and social development in Northeast China before 3,000 BC*. PhD Dissertation, Jilin University, Changchun. https://kns.cnki.net/KCMS/detail/detail.aspx?dbname=CDFDLAST2022&filename=1022426458.nh. Accessed 6 Aug 2024

Gilmore, C. C., & Grote, M. N. (2012). Estimating age from adult occlusal wear: A modification of the miles method. *American Journal of Physical Anthropology, 149*(2), 181–192. https://doi.org/10.1002/ajpa.22106

Górka, K., Romero, A., & Pérez-Pérez, A. (2016). Dental-macrowear and diet of Tigara foragers from Point Hope, northern Alaska. *Anthropologischer Anzeiger, 73*, 257–264. https://doi.org/10.1127/anthranz/2016/0613

Grine, F. E. (2002) Scaling of tooth enamel thickness, and molar crown size reduction in modern humans: Research letter. *South African Journal of Science*, *98*, 503—509. https://hdl.handle.net/10520/EJC97533. Accessed 6 Aug 2024

Grine, F. E. (2005). Enamel thickness of deciduous and permanent molars in modern *Homo sapiens*. *American Journal of Physical Anthropology, 126*, 14–31. https://doi.org/10.1002/ajpa.10277

He, L. T. (2015). *Stress for ancient population of Jiayi cemeteries in Turpan, Xinjiang Province*. Master's Dissertation, Jilin University, Changchun. https://kns.cnki.net/KCMS/detail/detail.aspx?dbname=CMFD201502&filename=1015589698.nh. Accessed 6 Aug 2024

Jiang, C. N. (2011). *Researches on the archaeological culture and ethnicity of Bronze Age in the Region of Gansu & Qinghai*. Master's Dissertation, Dongbei Normal University, Changchun. https://kns.cnki.net/KCMS/detail/detail.aspx?dbname=CMFD2012&filename=1012294136.nh. Accessed 6 Aug 2024

Jiang, H. E., Lv, E. G., & Zhang, Y. B. (2021). A consideration of the lifestyle of the ancient Yanghai people in Turpan. *Journal of the Turpan Studies*, *1*, 41–47+154. https://doi.org/10.14087/j.cnki.65-1268/k.2021.01.005

Kaifu, Y., Kasai, K., Townsed, G. C., & Richards, L. C. (2003). Tooth wear and the "design" of the human dentition: A perspective from evolutionary medicine. *American Journal of Physical Anthropology, 37*, 47–61. https://doi.org/10.1002/ajpa.10329

Kunikita, D., Wang, L. X., Onuki, S., Sato, H., & Matsuzaki, H. (2017). Radiocarbon dating and dietary reconstruction of the Early Neolithic Houtaomuga and Shuangta sites in the Song-Nen Plain, Northeast China. *Quaternary International, 441*, 62–68. https://doi.org/10.1016/j.quaint.2017.01.031

Li, C., Wu, Y., & Hou, X. (2011). Holocene vegetation and climate in Northeast China revealed from Jingbo Lake sediment. *Quaternary International, 229*(1–2), 67–73. https://doi.org/10.1016/j.quaint.2009.12.015

Li, Y., Li, X., Cao, H. Y., Li, C. C., Jiang, H. E., & Li, C. S. (2013). Grain remains from archaeological sites and development of oasis agriculture in Turpan, Xinjiang. *Chin Sci Bull, 58*(S1), 40–45. https://doi.org/10.1360/tb-2013-suppl017

Liu, J. (2020). *The social life of the former Yanghai people: Yanghai I cemetery from the Perspective of social archaeology*. Master's Dissertation, Xinjiang Normal University, Xinjiang: Urumqi. https://kns.cnki.net/KCMS/detail/detail.aspx?dbname=CMFD202102&filename=1021554648.nh. Accessed 6 Aug 2024

Liu, Y. M., Cao, J., & Wang, X. (2009). Study on nutritional compoents of Ta-er-mi from a traditional food of Kazakh in Xinjiang. *Science & Technology Food Industry*, *30*(3), 310–312. https://doi.org/10.13386/j.issn1002-0306.2009.03.093

Lovejoy, C. O. (1985). Dental wear in the Libben population: Its functional pattern and role in the determination of adult skeletal age at death. *American Journal of Physical Anthropology, 68*(1), 47–56. https://doi.org/10.1002/ajpa.1330680105

Lucas, P. W., & van Casteren, A. (2015). The wear and tear of teeth. *Medical Principles and Practice, 24*, 3–13. https://doi.org/10.1159/000367976

Macho, G. A., & Spears, I. R. (1999). Effects of loading on the biomechanical behavior of molars of *Homo*, *Pan*, and *Pongo*. *American Journal of Physical Anthropology*, *109*, 211–227. https://doi.org/10.1002/(SICI)1096-8644(199906)109:2<211::AID-AJPA6>3.0.CO;2-B

Mahoney P. M. (2013). Testing functional and morphological interpretations of enamel thickness along the deciduous tooth row in human children. *American Journal of Physical Anthropology*, *151*, 518–525. https://doi.org/10.1002/ajpa.22289

Mao, R. L., Yang, Y. G., & Jiang, C. N. (2017). The excavation of Dunping cemetery in Zhangxian County, Gansu in 2014. *Archaeology*, *8*, 35–51. https://kns.cnki.net/kcms/detail/detail.aspx?FileName=KAGU201708003&DbName=CJFQ2017. Accessed 6 Aug 2024

Mao, R. L., Yang, Y. G., Zhao, W. C., Fu, W. X., & Cao, X. X. (2019). The excavation of Dunping cemetery in Zhangxian County, Gansu in 2015. *Cultural Relics*, *3*, 19–37. https://doi.org/10.13619/j.cnki.cn11-1532/k.2019.03.002

Merrett, D. C., Zhang, H., Xiao, X., Zhang, Q., Wei, D., Wang, L., Zhu, H., & Yang, D. Y. (2016). Enamel hypoplasia in northeast China: Evidence from Houtaomuga. *Quaternary International, 405*, 11–21. https://doi.org/10.1016/j.quaint.2015.06.004
Miles, A. E. W. (2001). The miles method of assessing age from tooth wear revisited. *Journal of Archaeological Science, 28*, 973–982. https://doi.org/10.1006/jasc.2000.0652
Murphy, T. (1959). The changing pattern of dentin exposure in human tooth attrition. *American Journal of Physical Anthropology, 17*(3), 167–178. https://doi.org/10.1002/ajpa.1330170302
Richards, L. C., & Brown, T. (1981). Dental attrition and age relationships in Australian Aborignals. *Archaeology in Oceania, 16*, 94–98.
Romero, A., Ramírez-Rozzi, F. V., Cuesta-Torralvo, E., & Pérez-Pérez, A. (2019). Age-related tooth wear in African rainforest hunter-gatherers. *American Journal of Physical Anthropology, 170*(4), 622–628. https://doi.org/10.1002/ajpa.23934
Rose, J. C., & Ungar, P. S. (1998). Gross dental wear and dental microwear in historical perspective. In Alt, K. W., Rosing, F. W., Teschler Nicola, M. (Eds.). *Dental Anthropology: fundamentals, limits, prospects* (pp. 349–386) Gustav-Fischer. https://doi.org/10.1007/978-3-7091-7496-8_19
Schmidt, C. W. (2010). On the relationship of dental microwear to dental macrowear. *American Journal of Physical Anthropology, 142*(1), 67–73. https://doi.org/10.1002/ajpa.21197
Shao, X. Q. (1985). *Anthropometric manual*. Shanghai Lexicographical Publishing.
Smith, B. H. (1984). Patterns of molar wear in hunger-gatherers and agriculturalists. *American Journal of Physical Anthropology, 63*(1), 39–56. https://doi.org/10.1002/ajpa.1330630107
Smith, T. M., Olejniczaka, A. J., Reidc, D. J., Ferrelld, R. J., & Hublin, J. J. (2006). Modern human molar enamel thickness and enamel-dentine junction shape. *Archives of Oral Biology, 51*, 974–995. https://doi.org/10.1016/j.archoralbio.2006.04.012
Sun, Y. G., & Zhao, Z. J. (2013). A comprehensive study on the plant remains from Weijiawopu site of Hongshan culture. *Agricultural Archaeology, 3*, 1–5.
Sun, Y. G., Zhao, Z. J., & Ji, P. (2016). The research of plant remains from Haminmangha prehistorical settlement site. *Huaxia Archaeology*, *02*, 45–52. https://doi.org/10.16143/j.cnki.1001-9928.2016.02.006
Suo, X. F., & Li, S. B. (2013). Neolithic animal remains in Liaoxi area. *Steppe cultural relics*, *1*, 43–49. https://doi.org/10.16327/j.cnki.cn15-1361/k.2013.01.001
Teng H. (2013). The environmental changes and the rise and decline of "culture" — Taking the West Liaohe River Basin in North China as the research object. (环境变迁与"文化"的兴衰——以中国北方西辽河流域为考察对象). *Knowledge, 1*, 29–33. https://doi.org/10.16435/j.cnki.cn22-1273/c.2013.01.002
Wang, C. (2017). *Archaeobotanical studies at the Jiayi cemetery and naked barely processing of early Iron Age in east part of Xinjiang*. Master's Dissertation, University of Chinese Academy of Sciences, Beijing.
Wang, L. (2018). Studies on the remains of the Neolithic Age in Houtaomuga site and relevant issues. *Acta Archaeologica Sinica*, *2*, 141–164. https://kns.cnki.net/kcms/detail/detail.aspx?FileName=KGXB201802001&DbName=CJFQ2018. Accessed 6 Aug 2024
Wang, L., Xiao, G. Q., Liu, Z. J., Lv, E. G., & Wu, Y. (2014). Brief report on excavation of Jiayi cemeteries in Turpan, Xinjiang. *Journal of the Turpan Studies*, *1–19*, 157–161. https://doi.org/10.14087/j.cnki.65-1268/k.2014.01.015
Wu, R. K., Wu, X. Z., & Zhang, Z. B. (1984). *Anthropometric methods*. Science Press.
Xiao, X. M. (2014). *A research on the human skeletons of Houtaomuga site, Da'an City, Jilin Province*. Ph.D. Dissertation, Jilin University, Changchun. https://kns.cnki.net/KCMS/detail/detail.aspx?dbname=CDFDLAST2015&filename=1015504223.nh. Accessed 6 Aug 2024
Xiao, G. Q. (2018). *The review and study of Jia Yi Cemetery in Turfan, Xinjiang*. Master's Dissertation, Northwest University, Xi'an. https://kns.cnki.net/KCMS/detail/detail.aspx?dbname=CMFD201901&filename=1018119811.nh. Accessed 6 Aug 2024
Yang, J., & Cao, J. E. (2007). The culture development of ancient nomadic people in northern frontier of China. *Jilin University Journal of Social Science Edition*, *5*, 140–146. https://doi.org/10.15939/j.jujsse.2007.05.019
Zhang, X. L., Liu, G. X., Wang, M. H., & Lv, P. (2017a). Carbon and nitrogen stable isotope analysis of human skeletons unearthed from Xinglonggou site. *Cultural Relics in Southern China, 4*, 185–195. https://kns.cnki.net/kcms/detail/detail.aspx?FileName=LFWW201704030&DbName=CJFQ2017. Accessed 6 Aug 2024
Zhang, Q. C., Zhang, Q., & Han, T. (2017b). The stable isotope analysis of human skeletons from Banlashan cemetery, Chaoyang City, Liaoning province. In Xiong, Z. L., Fan, S. Y., Wu, Y. L., et al. (Eds.) *The excavation of Banlashan site of Hongshan archaeological culture in Chaoyang city,*

Liaoning Province (vol. 2, pp. 31–34+2) Archaeology. https://kns.cnki.net/kcms/detail/detail.aspx?FileName=KAGU201702001&DbName=CJFQ2017. Accessed 6 Aug 2024

Zhou, G. S., Wang, Y. H., & Jiang, Y. L. (2002). Global change and water-driven IGBP-NECT, northeast China. *Earth Science Frontiers*, *9*(1), 198–216. https://kns.cnki.net/kcms/detail/detail.aspx?FileName=DXQY200201038&DbName=CJFQ2002. Accessed 6 Aug 2024

Zhu, M. (2019). *The Neolithic Age settlement and social from evolution in the Nenjiang River Basin*. Master Dissertation, Liaoning Normal University, Shenyang. https://kns.cnki.net/KCMS/detail/detail.aspx?dbname=CMFD202001&filename=1019041217.nh. Accessed 6 Aug 2024

Authors and Affiliations

Shiyu Yang[1,2,7] · Laura M. Martínez[2,3] · Alejandro Romero[4] · Susana Carrascal[2,3,5] · Jie Guo[1] · Albert E. Dyowe[6] · Quanchao Zhang[1] · Alejandro Pérez-Pérez[2,3]

✉ Quanchao Zhang
py2000sdqy@sina.com

✉ Alejandro Pérez-Pérez
martinez.perez-perez@ub.edu

Shiyu Yang
yangshiyu2016@163.com

Laura M. Martínez
lmartinez@ub.edu

Alejandro Romero
arr@gcloud.ua.es

Susana Carrascal
susana.carrascal@gmail.com

Jie Guo
2890432476@qq.com

Albert E. Dyowe
albertepitie@gmail.com

1 School of Archaeology, Jilin University, Av. Qianjin 2699, 130012 Changchun, China

2 Dept. Biologia Evolutiva, Ecologia i Ciències Ambientals (BEECA), Universitat de Barcelona (UB), Av. Diagonal 643, 08028 Barcelona, Spain

3 Institut d'Arqueologia (IAUB), Universitat de Barcelona, Barcelona, Spain

4 Dept. Biotecnología, Universidad de Alicante (UA), Alicante, Spain

5 Dept. Biologia Animal, Biologia Vegetal i Ecologia (BABVE), Universitat Autònoma de Barcelona (UAB), Bellaterra, Spain

6 Dept. Prehistòria, Universitat Autònoma de Barcelona (UAB), Cerdanyola del Vallès, Spain

7 School of Archaeology and Literature, Chongqing Normal University, Av. 37 Daxuechenh Road, Shapinba, Chongqing 401331, China